Analysis of sound propagation in xenon near the critical point*

Dror Sarid
Xerox Corporation, Webster Research Center, Webster, New York 14580

David S. Cannell
Department of Physics and Quantum Institute, University of California at Santa Barbara, Santa Barbara, California 93106

(Received 6 May 1976)

Existing ultrasonic and light-scattering data on sound propagation are analyzed, both in terms of a relaxing viscosity as calculated by Kawasaki, and in terms of relaxing heat capacities as calculated by Mistura. The two theories are examined and found to be quite different, but neither theory is found to be capable of accounting for the data, although disagreement with Kawasaki's theory is much more pronounced. Although not in agreement with theory, a frequency-dependent viscosity very similar to that required to account for the observed ultrasonic dispersion and attenuation is found to yield anomalous Brillouin spectra in excellent agreement with those observed near the critical point.

I. INTRODUCTION

Considerable theoretical and experimental effort has been devoted to elucidating the dynamic behavior of fluids in the vicinity of their gas-liquid critical points. The decay of spontaneous entropy fluctuations has been studied extensively by means of light scattering, and in general both the mode-mode coupling theory of Kawasaki[1] and the decoupled mode theory of Ferrell[2] have been found to be in excellent accord with the data after corrections are made for background effects.[3] Measurement of the frequency and temperature dependence of the speed and attenuation of sound has also proved an excellent probe, and both ultrasonic measurements,[4-9] and Brillouin scattering measurements,[10-12] have been used in studying xenon.

Mode-mode coupling calculations have been used by Kawasaki[1] to compute the real and imaginary parts of a frequency-dependent viscosity $b_c(\omega)$ from which both the dispersion and attenuation may be predicted. Mistura[13] has obtained similar results by utilizing a complex frequency-dependent heat capacity. The physical mechanism responsible for the very large dispersion and attenuation observed is apparently much like a structural relaxation. The equilibrium long-range correlation is a function of density and temperature but requires time for its establishment, thus resulting in higher sound speeds at higher frequencies.

As Garland *et al.*[5] have shown, the expressions for the frequency-dependent viscosity or heat capacity may be cast in a particularly appealing form by the introduction of a dimensionless variable

$$\omega^* \equiv \omega \rho C_p \xi^2 / 2\Lambda , \tag{1}$$

where ω is the angular frequency, ρ the mass density, C_p the constant-pressure specific heat, Λ the thermal conductivity, and ξ is the long-range correlation length. The variable ω^* is π times the ratio of the time required for the decay of an entropy fluctuation of wave vector ξ^{-1}, to the period of the sound wave.

In terms of ω^* the real and imaginary parts of the critical contribution to the viscosity, $b_c(\omega)$, may be written

$$\omega \,\mathrm{Re} b_c(\omega) = D(T) I(\omega^*), \tag{2a}$$

$$\omega \,\mathrm{Im} b_c(\omega) = D(T) J(\omega^*), \tag{2b}$$

while the frequency-dependent excess heat capacity $\Delta(\omega)$ may be written

$$(1 - 1/\gamma) C_0^2 \,\mathrm{Re}[\Delta(\omega)]/C_V = -D(T) J(\omega^*), \tag{2c}$$

$$(1 - 1/\gamma) C_0^2 \,\mathrm{Im}[\Delta(\omega)]/C_V = D(T) I(\omega^*). \tag{2d}$$

Here C_0 is the zero-frequency sound speed, and $I(\omega^*)$ and $J(\omega^*)$ are functions of ω^* which may be calculated if one assumes a form for the density-density correlation function; $\gamma = C_p/C_V$, and $D(T)$ is given by

$$D(T) = \frac{k_B T^3}{\pi^2 \rho_0^3 C_V^2} \left(\frac{\partial P}{\partial T}\right)_V^2 \left[\xi^{-1} \left(\frac{\partial \xi^{-1}}{\partial T}\right)_S^2\right]. \tag{3}$$

Here k_B is Boltzmann's constant, T the absolute temperature, C_V the constant-volume specific heat, P the pressure, and S the entropy. Comparison with the theories is conveniently made by using the dispersion and attenuation data to compute $\mathrm{Re} b_c(\omega)$ and $\mathrm{Im} b_c(\omega)$ in the case of the Kawasaki theory, and $\mathrm{Re}\Delta(\omega)$ and $\mathrm{Im}\Delta(\omega)$ in the case of the Mistura theory. On the critical isochore $(\partial \xi^{-1}/\partial T)_S$ may be replaced[9] by $(\partial \xi^{-1}/\partial T)_\rho$. The term in brackets in Eq. (3) is quite sensitive to the temperature dependence of ξ, and the resulting uncertainties in $D(T)$ have made stringent experimental tests of the theory difficult. In fact,

$D(T)$ has often been treated as adjustable.

Although the theory of Mistura has generally been considered identical to that of Kawasaki, the fact that the equations used to link the calculated heat capacity[6] to the sound speed and attenuation are different from those used when dealing with the viscosity[14] actually make the two theories quite different, whenever there is appreciable dispersion. A careful study of the equations given in Refs. 6 and 14 shows this to be the case, but no detailed comparison of the two theories has been made before. In addition, previous analyses[9,11] have indicated a systematic difference between the results obtained from Brillouin scattering and those obtained from ultrasonic measurements. In carrying out these analyses Brillouin splittings and linewidths have been treated as equivalent to the results of an ultrasonic experiment performed at the Brillouin frequency, which is not justifiable *a priori*. In order to show clearly the large difference between the two theories and to investigate the effects of a more rigorous treatment of the Brillouin data, we have been led to reanalyze a portion of the existing data. By using the experimental data to compute the ratio $\mathrm{Im}b_c(\omega)/\mathrm{Re}b_c(\omega)$, in the case of the viscosity, and the ratio $-\mathrm{Re}\Delta(\omega)/\mathrm{Im}\Delta(\omega)$, in the case of the heat capacity, the theories may be tested without requiring knowledge of $D(T)$. The results of this test are in clear disagreement with the theory of Kawasaki using either the Ornstein-Zernike[15] or the Fisher-Langer[16] form of the correlation function, but are in good agreement with the theory of Mistura provided the Fisher-Langer form of the correlation function is used. The fact that the theory of Mistura does predict values for the ratio $-\mathrm{Re}\Delta(\omega)/\mathrm{Im}\Delta(\omega)$ which are in agreement with the ultrasonic results has been shown before in a rather different manner, because previous investigations[6,9,17] have shown that the choice of $D(T)$ which gave good agreement between the theory and the ultrasonic attenuation data also gave good agreement with the ultrasonic dispersion data. Our use of the Fisher-Langer form of the correlation function was motivated by the work of Tartaglia and Thoen,[17] who have shown that it leads to a significant improvement for large ω^*, over the results obtained using the Ornstein-Zernike form.

By making a particular choice for $D(T)$, which will be motivated below, we find that although there is fairly good agreement between the ultrasonic and Brillouin scattering data, especially for $\omega^* \gtrsim 10$, neither theory predicts the reduced dispersion and attenuation correctly; i.e., neither the values of $\mathrm{Re}\Delta(\omega)$ and $\mathrm{Im}\Delta(\omega)$ predicted by the Mistura theory, nor the values of $\mathrm{Re}b_c(\omega)$ and $\mathrm{Im}b_c(\omega)$ predicted by the Kawasaki theory, are in agreement with the data, although as mentioned, the theory of Mistura does predict the ratio $-\mathrm{Re}\Delta(\omega)/\mathrm{Im}\Delta(\omega)$ correctly.

The theory of Kawasaki gives results which are too small by as much as a factor of 10, while the theory of Mistura gives results which are too small by about a factor of 2. In the case of the Mistura theory, our findings are in agreement with those of Thoen and Garland,[9] who found that the values of $\xi^{-1}(\partial\xi^{-1}/\partial T)^2$, needed to fit the ultrasonic data on the critical isochore, were ~1.8 times larger than the values obtained using the best experimental values for ξ.

The quantity $\xi^{-1}(\partial\xi^{-1}/\partial T)^2$ is computed using an expression for ξ of the form $\xi_0 t^{-\nu}$, where $t=(T-T_c)/T_c$, and disagreement has previously been attributed to inadequate knowledge of ξ_0 and ν. In the course of performing our analysis we considered the effect of possible errors in ξ_0 and ν, such errors being higher correlated, and we find that there are in fact no reasonable choices for ξ_0 and ν which result in values of $\xi^{-1}(\partial\xi^{-1}/\partial T)^2$ sufficiently large to bring either theory into agreement with experiment. In fact, the choice of ξ_0 and ν presented below results in essentially the maximum possible values for $\xi^{-1}(\partial\xi^{-1}/\partial T)^2$. Since it is very unlikely that errors in other quantities could result in an error as large as a factor of 2, we conclude that neither theory is capable of accounting for the data.

In the course of this analysis we have also discovered that although not in agreement with theory, a frequency-dependent viscosity very similar to that required to account for the attenuation and dispersion of ultrasound in the critical region gives rise to a light scattering spectrum of exactly the form previously observed experimentally by one of us[10]; namely, the relaxing viscosity contributes significant spectral power in the frequency region between the Rayleigh and Brillouin components of the scattered light.

II. THEORY

A. Complex viscosity

This section outlines the modification of the Navier-Stokes equation which leads to a complex frequency-dependent viscosity, and reviews the effects of this modification on both the propagation of driven sound waves and on the spectrum of light scattered by the fluid. The use of a complex frequency-dependent volume viscosity offers a well-defined phenomenological approach to accounting for the effects of chemical reactions, energy transfer to internal states, and modifications in local structure, on the propagation of

acoustic waves.[18] This approach is equivalent to introducing an excess pressure which depends on the past history of the density. This may be seen by considering the linearized Navier-Stokes equation

$$\rho_0 \frac{\partial \vec{v}}{\partial t} = -\nabla P + \eta_s \nabla^2 \vec{v} + (\tfrac{1}{3}\eta_s + \eta_v)\nabla(\nabla \cdot \vec{v}) , \tag{4}$$

where ρ_0 is the average density, $\vec{v}$ the local velocity, and η_s and η_v are the shear and volume viscosities, respectively. The term $\eta_v \nabla(\nabla \cdot \vec{v})$ may be combined with the pressure term and $P - \eta_v \nabla \cdot \vec{v}$ regarded as an effective pressure. Using the linearized continuity equation

$$\frac{\partial \rho}{\partial t} + \rho_0 \nabla \cdot \vec{v} = 0 , \tag{5}$$

the effective pressure may be written

$$P_{\text{eff}} = P + \frac{\eta_v}{\rho_0} \frac{\partial \rho}{\partial t} . \tag{6}$$

In order to introduce "memory effects" we formally replace $(\eta_v/\rho_0)\,\partial\rho/\partial t$ by

$$\frac{1}{\rho_0} \int_0^\infty \eta_v(t') \dot{\rho}(t - t')\, dt' ,$$

where $\dot{\rho}(t - t')$ is the time derivative of ρ at $t - t'$. Thus $\eta_v(t')$ plays the role of a memory function, allowing density disturbances occurring at one time to contribute to the effective pressure at some later time,[19] the effective pressure being

$$P_{\text{eff}}(t) = P(t) + \frac{1}{\rho_0} \int_0^\infty \eta_v(t') \dot{\rho}(t - t')\, dt' . \tag{7}$$

The modified linearized Navier-Stokes equation then takes the form

$$\rho_0 \frac{\partial \vec{v}}{\partial t} = -\nabla P + \eta_s \nabla^2 \vec{v} + \tfrac{1}{3}\eta_s \nabla(\nabla \cdot \vec{v}) + \nabla \int_0^\infty \eta_v(t') \nabla \cdot \vec{v}(t - t')\, dt' . \tag{8}$$

Such a modification of the hydrodynamic equations affects both the propagation of driven sound waves and the spectrum of light scattered by the fluid, but in quite different ways. The three equations required to determine either the response to a sinusoidal driving force or the temporal response to an initial disturbance of a given wave vector are the continuity equation, Eq. (5), the modified linearized Navier-Stokes equation, Eq. (8), and the energy transport equation,

$$\rho_0 C_v \frac{\partial T}{\partial t} - \frac{C_v(\gamma - 1)}{\beta} \frac{\partial \rho}{\partial t} - \Lambda \nabla^2 T = 0 . \tag{9}$$

Here $\beta \equiv -(1/\rho_0)(\partial\rho/\partial T)_P$ is the thermal expansion coefficient, and Λ is the thermal conductivity. For the case of driven sound waves, one seeks a solution to these equations for which the deviations of the variables ρ, T, and $\vec{v}$ from their average values are of the form $e^{i(\vec{K}\cdot\vec{r} - \omega t)}$. The result is a set of homogeneous algebraic equations in ρ and T, after using the continuity equation to eliminate terms involving $\vec{v}$. The equations have nonzero solutions only if the following dispersion equation is satisfied[20]:

$$\omega^2/\vec{K}\cdot\vec{K} = C_0^2 + ab(\omega)(\vec{K}\cdot\vec{K}) - i\omega[a + b(\omega) - C_0^2 a(\vec{K}\cdot\vec{K})/\gamma\omega^2] . \tag{10}$$

Here C_0 is the zero-frequency sound speed, $a = \Lambda/\rho_0 C_v$, and the complex frequency-dependent viscosity $b(\omega)$ is given by

$$b(\omega) = [\tfrac{4}{3}\eta_s + \eta_v(\omega)]/\rho_0 \tag{11}$$

and

$$\eta_v(\omega) = \int_0^\infty \eta_v(t') e^{i\omega t'} dt' . \tag{12}$$

The spectrum of light scattered by such a fluid may be found by solving an initial-value problem for the temporal decay of a density disturbance of a given wave vector $\vec{k}$. As shown by Mountain[21] this is easily accomplished by taking the Laplace transform in time and the spatial Fourier transform of the three hydrodynamic equations, Eqs. (5), (8), and (9). The resulting algebraic equations may be solved exactly to obtain the spectrum of the scattered light, the result being

$$S(\vec{k}, \omega) \propto \text{Re}[F(s)/G(s)]_{s=i\omega} , \tag{13}$$

where s is the Laplace transform variable, and F and G are given by

$$F(s) = s^2 + [a + b(s)]k^2 s + ab(s)k^4 + C_0^2 k^2 (1 - 1/\gamma) , \tag{14a}$$

$$G(s) = s^3 + [a + b(s)]k^2 s^2 + [C_0^2 k^2 + ab(s)k^4]s + aC_0^2 k^4/\gamma . \tag{14b}$$

Here

$$b(s) = (1/\rho_0)[\tfrac{4}{3}\eta_s + \eta_v(s)] , \tag{15}$$

$$\eta_v(s) = \int_0^\infty e^{-st'} \eta_v(t')\, dt' . \tag{16}$$

This modification of the hydrodynamic equations affects sound propagation in a rather straightforward manner, but its effect on the spectrum is much more striking since for every internal process of relaxation time τ, $\eta_v(s)$ contains a term proportional to $(1 + s\tau)^{-1}$ which increases the order of F and G considered as polynomials in s, and this introduces a nonpropagating mode into the spectrum.[21] In the case of driven

sound waves, however, ω is real and $\vec{K}=\hat{n}(k_0+i\alpha)$ is complex. Here $k_0\equiv 2\pi/\lambda$, α is the amplitude attenuation coefficient, and $\hat{n}$ is a unit vector in the direction of propagation. In solving the dispersion equation for $\vec{K}$ in terms of ω, the algebraic structure of the equation is unaffected by the frequency dependence of $b(\omega)$ and thus no new modes appear.

As pointed out previously[14] for the case of driven sound waves, the dispersion equation may be solved exactly for both the real and imaginary parts of $b(\omega)$ in terms of the sound speed $C(\omega)$ and the amplitude attenuation per wavelength $\alpha\lambda(\omega)$. Thus measurements of $C(\omega)$ and $\alpha\lambda(\omega)$ yield $b(\omega)$ directly. The exact expression for $b(\omega)$ is complicated and not very instructive, but the approximate solutions

$$\omega\,\mathrm{Re}b(\omega)=\frac{2\bar{\alpha}C^2(\omega)}{(1+\bar{\alpha}^2)^2}\,, \tag{17a}$$

$$\omega\,\mathrm{Im}b(\omega)=C^2(\omega)\frac{1-\bar{\alpha}^2}{(1+\bar{\alpha}^2)^2}-C_0^2\,, \tag{17b}$$

where $\bar{\alpha}=\alpha\lambda/2\pi$, proved accurate to a few percent when applied to SF_6 near its critical point, even when $\alpha\lambda$ was as large as unity.[14] Equations (17) give the real and imaginary parts of the total viscosity, while the theory gives only the critical contributions. The contributions of the shear viscosity and the nonrelaxing part of the volume viscosity, if any, are to be subtracted directly from the experimental values for $\mathrm{Re}b(\omega)$ before comparison with theory. These contributions are negligible for the ultrasonic data.

Kawasaki has used a mode-mode coupling approach to calculate the frequency dependence of both the real and imaginary parts of the viscosity, and Garland *et al.*[5] have shown that his result may be written very elegantly by using the reduced frequency ω^* discussed in the Introduction. The results have been given in Eqs. (2a) and (2b), where the integrals $I(\omega^*)$ and $J(\omega^*)$ are given by

$$I(\omega^*)=\int_0^\infty dx\,\frac{x^2}{(1+x^2)^2}\,\frac{\omega^* K(x)}{\omega^{*2}+K^2(x)}\,, \tag{18a}$$

$$J(\omega^*)=\int_0^\infty dx\,\frac{x^2}{(1+x^2)^2}\,\frac{\omega^{*2}}{\omega^{*2}+K^2(x)}\,. \tag{18b}$$

In these expressions $K(x)$ is $\frac{3}{4}[1+x^2+(x^3-x^{-1})\tan^{-1}x]$, and the Ornstein-Zernike correlation function has been used in obtaining the expressions for $I(\omega^*)$ and $J(\omega^*)$.

The common prefactor of $I(\omega^*)$ and $J(\omega^*)$ in Eqs. (2) which we denote by $D(T)$ is rather sensitive to the density and temperature dependence of ξ, and this has made accurate comparison of the theory and data very difficult. Since, however, $\omega\,\mathrm{Re}b(\omega)$ and $\omega\,\mathrm{Im}b(\omega)$ can be computed fairly accurately from measurements of $C(\omega)$ and $\alpha\lambda(\omega)$ using Eqs. (17), one can remove all consideration of the prefactor $D(T)$ by computing the ratio

$$R=\mathrm{Im}b_c(\omega)/\mathrm{Re}b_c(\omega) \tag{19}$$

from the data as a function of ω^* and comparing it to the values computed from the expressions for $I(\omega^*)$ and $J(\omega^*)$ using various forms of the correlation function. Obviously this test of the theory is less complete than could be obtained with accurate knowledge of $D(T)$ but given realistic constraints on the accuracy with which $D(T)$ may be computed this method does provide a clear-cut test. In order to compute ω^*, one does need values for ξ and $\Lambda/\rho C_p$; however, the results of this test are nearly independent of the values assumed, for any reasonable choices. The values presented in the section on data analysis result in the quantity $2\Lambda/\rho C_p\xi^2$ being given by the expression $3.52\times 10^{12}t^{2.01}$, which is intermediate to the expressions used in Refs. 6 and 9. The ratio R as a function of ω^* for two different choices of the correlation function is shown in Fig. 4 in the data analysis section. It is rather remarkable that the Ornstein-Zernike correlation function results in the very simple expression $R=1.0\omega^{*0.348}$ in the range $1.0<\omega^*<10^5$, but it is not obvious why this should be so.

B. Complex heat capacity

Mistura[13] and Garland *et al.*[5] have developed an expression for a complex frequency-dependent excess specific heat, $\Delta(\omega)$, which is very similar to Kawasaki's expression for the viscosity. These results may also be written in terms of ω^* as given by Eqs. (2c) and (2d). The dispersion equation used to relate the excess heat capacity to the sound speed and critical attenuation[6] can be written

$$\frac{\omega^2}{\vec{K}\cdot\vec{K}}=C_0^2\frac{1+\Delta/C_p}{1+\Delta/C_v}\,, \tag{20}$$

which is based on the assumption that the excess heat capacity contributes equally to C_p and C_v. It should also be noted that this approach assumes that the critical dispersion and attenuation may be described without allowing for both classical and critical effects simultaneously in a full hydrodynamic theory as was done in the case of the viscosity. The critical attenuation is computed by subtracting the classical contributions from the Brillouin linewidths, and is set equal to the total observed attenuation for the ultrasonic results. As in the case of the viscosity one may solve exactly for the real and imaginary parts of $\Delta(\omega)$ in terms of $C(\omega)$ and $\bar{\alpha}_c$, where $\bar{\alpha}_c\equiv[\alpha\lambda(\omega)]_c/2\pi$

is the "critical attenuation per wavelength" divided by 2π. For $\gamma \neq 1$ and $\bar{\alpha}_c^2 \ll 1$, the exact solutions are very well approximated by the following expressions:

$$\frac{\mathrm{Im}\Delta(\omega)}{C_v} = \frac{2\bar{\alpha}_c C_0^2 C^2(\omega)(1-1/\gamma)}{[C^2(\omega) - C_0^2/\gamma]^2}, \tag{21a}$$

$$\frac{\mathrm{Re}\Delta(\omega)}{C_v} = \frac{C_0^2 - C^2(\omega)}{C^2(\omega) - C_0^2/\gamma}. \tag{21b}$$

These equations become identical to those given by Eden *et al.*[6] when $C^2(\omega)/C_0^2 \to 1$ (far from T_c), or when $\gamma^{-1} \to 0$ (near T_c).

We have not attempted to derive an expression for the spectrum of light scattered by a fluid with such an excess heat capacity, nor have we attempted to include the effects of viscous dissipation and heat conduction in a complete hydrodynamic theory as was done for the viscosity. When more accurate data for the correlation range make stringent comparison of this theory with the data possible, it will be necessary to carry out both of these calculations. Obviously the same ratio test may be applied to this theory; $\mathrm{Im}\Delta(\omega)/C_v$ and $\mathrm{Re}\Delta(\omega)/C_v$ can be obtained from the data using Eqs. (21), and from Eqs. (2c) and (2d) the ratio $-\mathrm{Re}\Delta(\omega)/\mathrm{Im}\Delta(\omega)$ may be compared directly to $J(\omega^*)/I(\omega^*)$.

III. DATA ANALYSIS

This section presents an analysis of a fraction of the available ultrasonic data[7] on sound speed and attenuation, and also presents an analysis of the results of detailed measurements[10] of the Brillouin spectrum. All data considered were taken on the critical isochore ($\rho = \rho_c$, $T > T_c$). The zero-frequency sound speed was taken from the 1-kHz measurements of Garland and Williams.[8] The analysis was carried out for the case of a relaxing viscosity and for the case of relaxing heat capacities. The analysis in the case of the viscosity is complete in the sense that the effects of thermal conduction and classical viscous dissipation are handled in a rigorous manner, and the Brillouin data are also handled rigorously and not treated as though equivalent to the results of an ultrasonic experiment at the Brillouin frequency.

Although the clearest test of the theories is carried out using the ratio test described in the previous section, it is also of some interest to choose a best estimate for the behavior of the long-range correlation length and use this to calculate $D(T)$, so that the dispersion data and the attenuation data may be compared separately to the theoretical predictions. As mentioned previously, these comparisons are rather sensitive to the magnitude and temperature dependence of ξ. Table I summarizes the thermodynamic data used to calculate both $D(T)$ and ω^*, and was taken from Swinney and Henry's[3] compilation of various experimental results. Other than ξ, these quantities are rather accurately known for $T - T_c \leq 5$ K. Since only four of the light scattering data points and none of the ultrasonic data correspond to $T - T_c > 5$ K, additional uncertainties far from T_c should not affect our conclusions. The evidence with regard to ξ may be summarized as follows. It has been very accurately measured on the critical isochore for CO_2 and SF_6 by one of us[22,23] and the two results are given by

$$\xi_{CO_2} = 56.0(T - T_c)^{-0.633 \pm 0.01}\ \text{Å},$$

$$\xi_{SF_6} = 72.44(T - T_c)^{-0.621 \pm 0.01}\ \text{Å}.$$

Both Giglio and Benedek[24] and Smith, Giglio, and Benedek[25] have measured ξ for xenon using essentially the same apparatus for both experiments and found the result

$$\xi_{Xe} = 80.4(T - T_c)^{-0.58 \pm 0.05}\ \text{Å},$$

but the expression $71(T - T_c)^{-0.63}$ is also in excellent agreement[3] with their data, and is much more in accord with the results for the other fluids. In fact, if one excludes from the analysis their point obtained at $T - T_c = 22$ mK which was probably influenced by multiple scattering[22] and also excludes the four points taken for $T - T_c > 0.47$ K because of the large uncertainties, the remaining 11 data points yield the least-mean-square fit

$$\xi_{Xe} = 75.6(T - T_c)^{-0.62}\ \text{Å},$$

when weighted equally, which is in close accord with the results for SF_6 and CO_2. For these reasons we have used the expression given in Table I in computing ξ.

The ultrasonic and light scattering data used

TABLE I. Thermodynamic data[a] used to calculate $D(T)$ and ω^*.

$\left(\frac{\partial P}{\partial T}\right)_v = 1.194\times10^6 + 5.54\times10^3(T-T_c)^{0.92} - 1.76\times10^3(T-T_c)^{1.14}$ dyn/cm² K
$\xi = 71(T-T_c)^{-0.63}$ Å
$C_v = [4.725(T-T_c)^{-0.146} - 1.525]\times10^6$ erg/g K
$C_p = 4.41\times10^8(T-T_c)^{-1.21}$ erg/g K
$\frac{\Lambda}{\rho C_p} = 1.01\times10^{-5}(T-T_c)^{0.748}$ cm²/sec
$\eta_s = 549 + 0.756(T-T_c) - 16.35\ \ln(T-T_c)$ μP

[a] These data, obtained by various authors, appear in H. L. Swinney and D. L. Henry Phys. Rev. A 8, 2586 (1973).

TABLE II. Brillouin scattering[a] and 1-kHz ultrasonic data[b] used in the analysis.

$T-T_c$ (K)	C_0 (m/sec)	C (m/sec)	$\bar{\alpha}$
0.10	85.0	123.7	0.100
0.20	90.0	124.3	0.099
0.30	93.7	127.3	0.097
0.40	96.6	124.5	0.099
0.50	99.0	126.8	0.094
0.70	102.6	124.3	0.095
1.03	106.8	126.8	0.091
2.24	117.4	128.9	0.080
3.00	121.8	132.7	0.073
5.00	130.0	134.3	0.062
7.50	136.8	140.5	0.051
10.00	142.6	146.7	0.040
15.00	152.0	152.4	0.032
20.00	159.7	162.4	0.027

[a] D. S. Cannell and G. B. Benedek, Phys. Rev. Lett. 25, 1157 (1970).

[b] C. W. Garland and R. D. Williams, Phys. Rev. A 10, 1328 (1974).

in the analysis are presented in Tables II and III. In carrying out the analysis in terms of the viscosity, the nonrelaxing part of the volume viscosity, η_{v0}, was set equal to η_s, and the contributions due to η_s and η_{v0} were subtracted from the computed values of $\mathrm{Re}b(\omega)$. The values of $\omega\,\mathrm{Re}b_c(\omega)/D(T)$ and $\omega\,\mathrm{Im}b_c(\omega)/D(t)$ as functions of ω^* are presented in Figs. 1 and 2, together with the theoretical expressions for $I(\omega^*)$ and $J(\omega^*)$ computed using both the Ornstein-Zernike and the Fisher-Langer form of the correlation function.[17] The symbols corresponding to the Brillouin data are the results obtained treating it as ultrasonic data. Since treating the Brillouin scattering results in this fashion is not justified, a smooth curve was fitted through the results obtained from the Brillouin data for $\omega\,\mathrm{Im}b_c(\omega)/D(T)$ and $\omega\,\mathrm{Re}b_c(\omega)/D(T)$, and used to compute $b_c(\omega)$ at any desired temperature in order to generate the expected spectra using Eqs. (13) and (14). The resulting spectra were not equal to those observed to within experimental accuracy, so the curves used to compute $b_c(\omega)$ were corrected and this procedure was repeated until the resulting spectra reproduced the observed splittings and linewidths to within experimental accuracy for all temperatures.

The final curves obtained in this way are shown as dashed lines in Figs. 1 and 2, and actually represent the correct determination of $\omega\,\mathrm{Re}b_c(\omega)/D(T)$, and $\omega\,\mathrm{Im}b_c(\omega)/D(T)$ corresponding to the Brillouin data. It is seen that the observed splittings may be used to compute $\omega\,\mathrm{Im}b_c(\omega)/D(T)$ to within experimental accuracy, but that the observed linewidths when treated as equivalent to ultrasonic results yield values for $\omega\,\mathrm{Re}b_c(\omega)/D(T)$ which are as much as 20% too large. The linewidths and splittings used in this analysis were obtained by solving the dispersion equation $G(s)=0$ corresponding to the spectra after deconvolution from the instrumental response.[10,19] The imaginary parts of the complex roots are $\pm Ck$, and the real parts are the negative of the Brillouin linewidths.

One very interesting result of this analysis is that the spectra generated in this manner reproduced not only the observed Brillouin splittings and linewidths but also duplicated rather accurately the spectral power present in the frequency region between the Rayleigh and Brillouin components. This is shown in Fig. 3, which presents both the experimentally observed spectrum, after deconvolution from the instrumental response,[19] and the one generated using the frequency-dependent vis-

TABLE III. Ultrasonic[a] and 1-kHz ultrasonic data[b] used in the analysis.

		1 MHz		3 MHz	
$T-T_c$ (K)	C_0 (m/sec)	C (m/sec)	$\bar{\alpha}$	C (m/sec)	$\bar{\alpha}$
0.050	81.0	96.22	0.063	101.81	0.068
0.062	82.2	96.30	0.062	103.10	0.066
0.075	83.4	96.12	0.061	103.10	0.075
0.082	83.9	96.37	0.056	103.09	0.058
0.183	89.2	98.21	0.045	100.37	0.056
0.283	93.1	99.84	0.036	100.71	0.048
0.383	96.1	101.25	0.030	103.52	0.043
0.482	98.7	102.51	0.026	104.62	0.037
0.582	100.7	103.96	0.021	105.20	0.033
0.682	102.3	105.14	0.019	105.95	0.031
0.782	103.8	106.28	0.016	107.66	0.026

[a] P. E. Mueller, D. Eden, C. W. Garland, and R. C. Williamson, Phys. Rev. A 6, 2272 (1972).

[b] C. W. Garland and R. D. Williams, Phys. Rev. A 10, 1328 (1974).

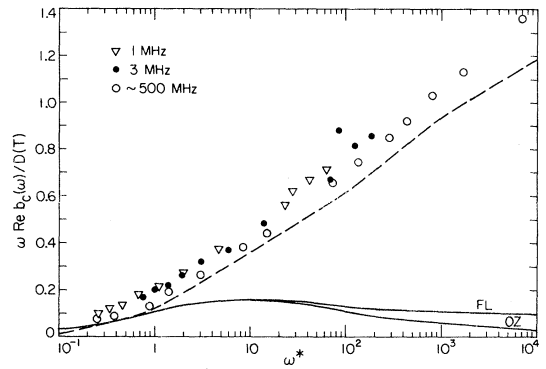

FIG. 1. $\omega\,\mathrm{Re}b_c(\omega)/D(T)$ vs ω^* for xenon near its critical point. The dashed line shows the values which result in spectra in agreement with the observed Brillouin spectra, while the open circles show the results of treating the Brillouin data as equivalent to the results of an ultrasonic experiment at the Brillouin frequency. The solid curves give the theoretical results from the mode-mode coupling theory using the Ornstein-Zernike and the Fisher-Langer forms of the correlation function.

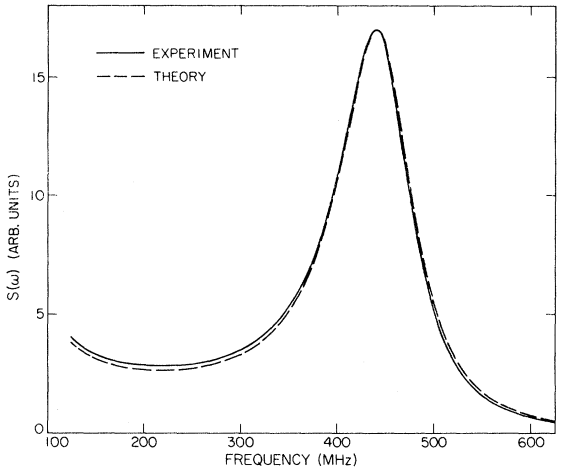

FIG. 3. Comparison of the Brillouin spectrum at $T - T_c = 0.2$ K after deconvolution from the instrumental response, and the spectrum computed using the frequency-dependent viscosity given by the dashed lines in Figs. 1 and 2.

cosity, at $T - T_c = 0.2$ K. The agreement is quite remarkable.

The discrepancies between the values for $\omega\,\mathrm{Re}b_c(\omega)/D(T)$ and $\omega\,\mathrm{Im}b_c(\omega)/D(T)$ obtained using the ultrasonic data and the Brillouin data are at the upper limit of what can reasonably be attributed to experimental error. Of course, if one were to adjust $D(T)$ by varying the expression used to compute $\xi^{-1}(\partial\xi^{-1}/\partial T)_\rho^2$ the agreement could be improved, but as will be seen, the data cannot be brought into agreement in this way. The discrepancy between the computed values of $\omega\,\mathrm{Re}b_c(\omega)/D(T)$ and $I(\omega^*)$ is outside any possibility of experimental error even allowing for reasonable errors in $D(T)$, and the agreement between $\omega\,\mathrm{Im}b_c(\omega)/D(T)$ and $J(\omega^*)$ is not much better.

Figure 4 shows the ratio $\mathrm{Im}b_c(\omega)/\mathrm{Re}b_c(\omega)$ as determined from the data and as given by the theoretical expressions for $I(\omega^*)$ and $J(\omega^*)$ using both the Ornstein-Zernike and the Fisher-Langer correlation functions. The dashed line in Fig. 4 is the ratio as determined from the dashed lines in Figs. 1 and 2, and represents the ratio as determined by a rigorous treatment of the Brillouin data. The agreement between the ultrasonic and Brillouin scattering results is only fair, and may show that when analyzed in this manner the real and imaginary parts of the viscosity are not universal functions of ω^*. Since $D(T)$ plays no role in the ratio, the disagreement between the data and the theory cannot be due to any error in determining $D(T)$.

The analysis in terms of relaxing heat capacities

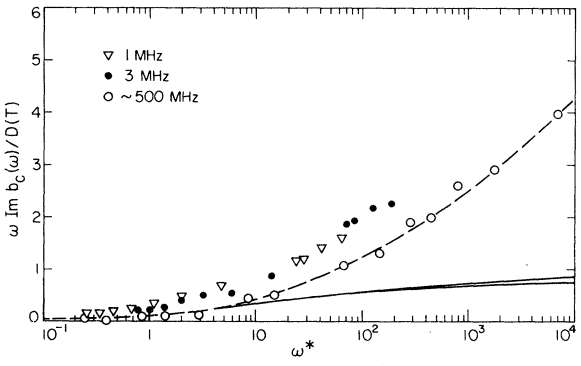

FIG. 2. $\omega\,\mathrm{Im}b_c(\omega)/D(T)$ vs ω^* for xenon near its critical point. The dashed and solid lines are as explained in the caption to Fig. 1.

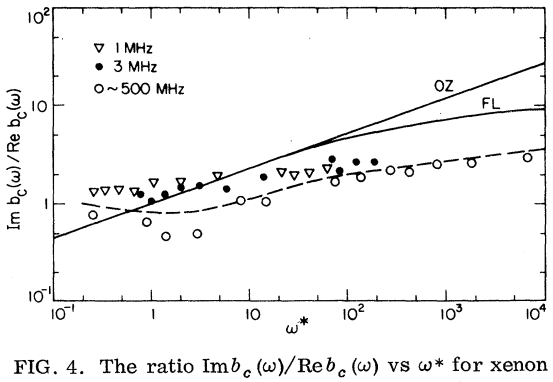

FIG. 4. The ratio $\mathrm{Im}b_c(\omega)/\mathrm{Re}b_c(\omega)$ vs ω^* for xenon near its critical point. The dashed and solid lines are the ratios corresponding to the dashed and solid lines in Figs. 1 and 2.

was carried out using Eqs. (21) to compute the real and imaginary part of the excess heat capacity $\Delta(\omega)$. According to the theory of Mistura[13] and Garland *et al.*,[5] the real and imaginary parts of $\Delta(\omega)$ are related to $I(\omega^*)$ and $J(\omega^*)$ by Eqs. (2c) and (2d). The values of $-(1-1/\gamma)C_0^2\mathrm{Re}\Delta(\omega)/C_vD(T)$ and $(1-1/\gamma)C_0^2\mathrm{Im}\Delta(\omega)/C_vD(T)$ computed from the data are shown in Figs. 5 and 6, respectively, where they may be compared to the theoretical curves obtained using the Ornstein-Zernike and the Fisher-Langer correlation functions. When one considers the possibility of errors in $D(T)$, the results of both light scattering and ultrasonic measurements may be considered to be in fairly good agreement with each other. Of course some change presumably would occur in the results for $\mathrm{Im}\Delta(\omega)$ obtained from the Brillouin scattering measurements if one were to generate spectra using a frequency-dependent heat capacity, and adjust $\mathrm{Re}\Delta(\omega)$ and $\mathrm{Im}\Delta(\omega)$ to obtain accurate spectra, but judging from the results found in the viscosity analysis the changes will not be too large, and it does not seem worthwhile to do this until accurate values for ξ are known.

The results of computing the ratio $-\mathrm{Re}[\Delta(\omega)]/\mathrm{Im}[\Delta(\omega)]$ from the data are shown in Fig. 7, and are seen to be in excellent agreement with the ratio $J(\omega^*)/I(\omega^*)$ computed using the Fisher-Langer correlation function. As shown in Figs. 5 and 6, however, neither the real nor the imaginary part of $\Delta(\omega)$ is in agreement with theory, for the choice of $D(T)$ used here. Since most of the uncertainty in $D(T)$ arises from lack of precise knowledge of ξ, we attempted to improve the agreement between the data and theory by adjusting the values of ξ_0 and ν in the expression $\xi = \xi_0(T-T_c)^{-\nu}$. We find that there are no choices for ξ_0 and ν which bring the data and theory into agreement and are even marginally consistent with the data for ξ. In fact, the expression for ξ presented in Table I results in essentially the maximum possible values for $D(T)$. Thus we conclude that although the theory involving relaxation of the heat capacity does correctly predict the ratio of reduced dispersion to reduced attenuation, it does not correctly predict either the reduced dispersion or the reduced attenuation, being too small in both cases by approximately a factor[26] of 2 for the larger values of ω^*. This conclusion differs from that of Eden and Swinney[12] because they only considered data for values of $\omega^* \leq 2$ where the discrepancies are not observable.

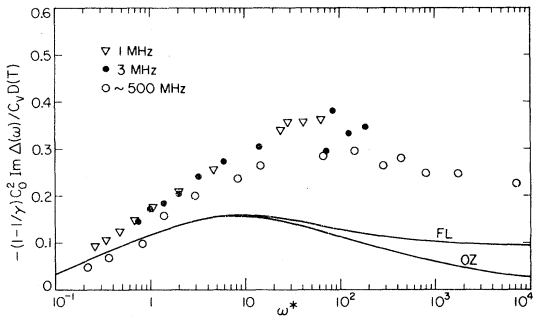

FIG. 6. $(1-1/\gamma)C_0^2\mathrm{Im}\Delta(\omega)/C_vD(T)$ vs ω^* for xenon near its critical point. The solid lines are the theoretical results.

IV. CONCLUSIONS

We have shown by means of detailed comparison, that the mode-mode coupling theory of Kawasaki utilizing a frequency-dependent viscosity and the theory of Mistura involving a relaxation of the heat capacities are actually quite different, a fact which we do not feel has been widely appreciated. We also find that neither theory is capable of adequately accounting for the dispersion and attenuation of

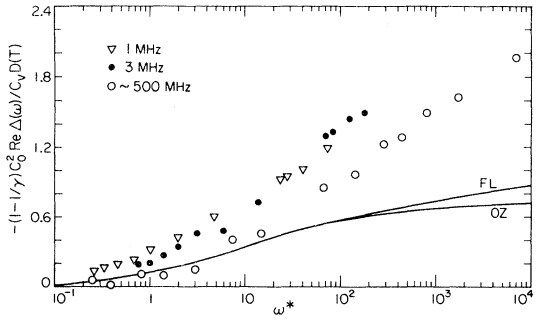

FIG. 5. $-(1-1/\gamma)\,C_0^2\,\mathrm{Re}\Delta(\omega)/C_vD(T)$ vs ω^* for xenon near its critical point. The solid curves give the theoretical results from the relaxing heat capacity theory of Mistura.

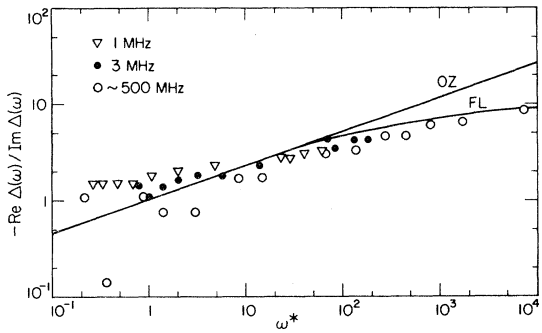

FIG. 7. The ratio $-\mathrm{Re}\Delta(\omega)/\mathrm{Im}\Delta(\omega)$ vs ω^* for xenon near its critical point. The solid curves are the ratios of the solid curves in Figs. 5 and 6.

sound observed near the critical point of xenon, but unlike previous workers we find that this cannot be attributed to uncertainty in the experimental results for the long-range correlation length. We do find, however, that the theory of Mistura is capable of accounting for the ratio of reduced dispersion to reduced attenuation for both light scattering and ultrasonic data provided the Fisher-Langer form of the correlation function is employed. This conclusion agrees with those of previous workers for the ultrasonic case. We also find that a frequency-dependent viscosity very similar to that required to account for the dispersion and attenuation observed at ultrasonic frequencies results in Brillouin spectra of the anomalous form observed near the critical point.

ACKNOWLEDGMENT

One of us (D.S.) would like to extend his sincere appreciation to the Quantum Institute of the University of California at Santa Barbara for the support and hospitality which made the work reported here possible.

---

*Research supported by the National Science Foundation and the Quantum Institute of the University of California, Santa Barbara, California.

[1]K. Kawasaki, Phys. Lett. 30A, 325 (1969); Ann. Phys. (New York) 61, 1 (1970); Phys. Rev. A 1, 1750 (1970).
[2]R. A. Ferrell, Phys. Rev. Lett. 24, 1169 (1970).
[3]H. L. Swinney and D. L. Henry, Phys. Rev. A 8, 2586 (1973).
[4]J. L. Kline and E. F. Carome, J. Chem. Phys. 58, 4962 (1973).
[5]C. W. Garland, D. Eden, and L. Mistura, Phys. Rev. Lett. 25, 1161 (1970).
[6]D. Eden, C. W. Garland, and J. Thoen, Phys. Rev. Lett. 28, 726 (1972).
[7]P. E. Mueller, D. Eden, C. W. Garland, and R. C. Williamson, Phys. Rev. A 6, 2272 (1972).
[8]C. W. Garland and R. D. Williams, Phys. Rev. A 10, 1328 (1974).
[9]J. Thoen and C. W. Garland, Phys. Rev. A 10, 1311 (1974).
[10]D. S. Cannell and G. B. Benedek, Phys. Rev. Lett. 25, 1157 (1970).
[11]H. Z. Cummins and H. L. Swinney, Phys. Rev. Lett. 25, 1165 (1970).
[12]D. Eden and H. L. Swinney, Opt. Commun. 10, 191 (1974).
[13]L. Mistura, in *Proceedings of the Enrico Fermi International School of Physics: Critical Phenomena*, edited by M. S. Green (Academic, New York, 1971), p. 563.
[14]D. S. Cannell and D. Sarid, Phys. Rev. A 10, 2280 (1974).
[15]L. S. Ornstein and F. Zernike, Proc. Acad. Sci. Amsterdam 17, 793 (1914); Z. Phys. 19, 134 (1918).
[16]M. E. Fisher and J. S. Langer, Phys. Rev. Lett. 20, 665 (1968).
[17]P. Tartaglia and J. Thoen, Phys. Rev. A 11, 2061 (1975). The values for $I(\omega^*)$ and $J(\omega^*)$ were obtained from the curves labeled FL_2 in this reference.
[18]L. D. Landau and E. M. Lifshitz, *Fluid Mechanics*, (Addison-Wesley, Reading, Mass., 1959), p. 304ff.
[19]D. S. Cannell, Ph.D. thesis (Physics Department, Massachusetts Institute of Technology, 1970) (unpublished).
[20]S. R. De Groot and P. Mazur, *Non Equilibrium Thermodynamics* (North-Holland, Amsterdam, 1963), p. 316.
[21]R. D. Mountain, J. Res. Natl. Bur. Stand. 70A, 207 (1966).
[22]J. H. Lunacek and D. S. Cannell, Phys. Rev. Lett. 27, 841 (1971).
[23]D. S. Cannell, Phys. Rev. A 12, 225 (1975).
[24]M. Giglio and G. B. Benedek, Phys. Rev. Lett. 23, 1145 (1969).
[25]I. W. Smith, M. Giglio, and G. B. Benedek, Phys. Rev. Lett. 27, 1556 (1971).
[26]In this regard it should be noted that the expression for $\Delta(\omega)$ given by Eq. (4) of Ref. 5 and Eq. (18) of Ref. 13 is too large by a factor of 2, but the expressions obtained in Refs. 6, 9, and 17 for the attenuation and dispersion are correct.